International Journal of Radiation Oncology biology • physics

www.redjournal.org

Biology Contribution

Physiological Interaction of Heart and Lung in Thoracic Irradiation

Ghazaleh Ghobadi, MSc,[*,†] Sonja van der Veen, MD,[*,†] Beatrijs Bartelds, MD, PhD,[‡] Rudolf A. de Boer, MD, PhD,[§] Michael G. Dickinson, MD,[‡] Johan R. de Jong, PhD,[‖] Hette Faber,[*,†] Maarten Niemantsverdriet, PhD,[*,†] Sytze Brandenburg, PhD,[¶] Rolf M.F. Berger, PhD,[‡] Johannes A. Langendijk, MD, PhD,[*] Robert P. Coppes, PhD,[*,†] and Peter van Luijk, PhD[*]

*Departments of *Radiation Oncology and †Cell Biology, ‡Center for Congenital Heart Disease, Beatrix Children Hospital, Departments of §Cardiology and ‖Nuclear Medicine and Molecular Imaging, University of Groningen, University Medical Center Groningen, and ¶Kernfysisch Versneller Instituut, University of Groningen, Groningen, The Netherlands*

Received Feb 21, 2012, and in revised form Jul 16, 2012. Accepted for publication Jul 20, 2012

Summary

Coirradiation of the heart enhances risk and severity of radiation-induced lung toxicity through an unknown mechanism. We show that irradiation of heart, lung, or both independently induces specific cardiac dysfunction and pulmonary vascular damage, mutually enhancing each other. These results show that treatment of thoracic cancer with radiation therapy requires optimization for both pulmonary and cardiac function to reduce the risk of toxicity.

Introduction: The risk of early radiation-induced lung toxicity (RILT) limits the dose and efficacy of radiation therapy of thoracic tumors. In addition to lung dose, coirradiation of the heart is a known risk factor in the development RILT. The aim of this study was to identify the underlying physiology of the interaction between lung and heart in thoracic irradiation.

Methods and Materials: Rat hearts, lungs, or both were irradiated to 20 Gy using high-precision proton beams. Cardiopulmonary performance was assessed using breathing rate measurements and F^{18}-fluorodeoxyglucose positron emission tomography (^{18}F-FDG-PET) scans biweekly and left- and right-sided cardiac hemodynamic measurements and histopathology analysis at 8 weeks postirradiation.

Results: Two to 12 weeks after heart irradiation, a pronounced defect in the uptake of ^{18}F-FDG in the left ventricle (LV) was observed. At 8 weeks postirradiation, this coincided with LV perivascular fibrosis, an increase in LV end-diastolic pressure, and pulmonary edema in the shielded lungs. Lung irradiation alone not only increased pulmonary artery pressure and perivascular edema but also induced an increased LV relaxation time. Combined irradiation of lung and heart induced pronounced increases in LV end-diastolic pressure and relaxation time, in addition to an increase in right ventricle end-diastolic pressure, indicative of biventricular diastolic dysfunction. Moreover, enhanced pulmonary edema, inflammation and fibrosis were also observed.

Conclusions: Both lung and heart irradiation cause cardiac and pulmonary toxicity via different mechanisms. Thus, when combined, the loss of cardiopulmonary performance is intensified further, explaining the deleterious effects of heart and lung coirradiation. Our

Reprint requests to: Peter van Luijk, PhD, Department of Radiation Oncology, University Medical Center Groningen, University of Groningen, PO Box 30001, 9700 RB, Groningen, The Netherlands. Tel: (+31) 50-3611739; Fax: (+31) 50-3611692; E-mail: p.van.luijk@umcg.nl

Authors RPC and PvL contributed equally to this work.

This work was funded by the Dutch Cancer Society (Grant No. RUG: 2007-3890) and the Innovational Research Incentives Scheme of the Netherlands Organization for Scientific Research (Grant No. 916.76.029).

Conflict of interest: none.

Supplementary material for this article can be found at www.redjournal.org.

Int J Radiation Oncol Biol Phys, Vol. 84, No. 5, pp. e639–e646, 2012
0360-3016
http://dx.doi.org/10.1016/j.ijrobp.2012.07.2362

findings show for the first time the physiological mechanism underlying the development of a multiorgan complication, RILT. Reduction of dose to either of these organs offers new opportunities to improve radiation therapy treatment of thoracic tumors, potentially facilitating increased treatment doses and tumor control.

Introduction

For many thoracic tumors treated with radiation therapy, dose escalation is expected to improve local control. However, the dose that can be administered safely is limited by the risk of potentially lethal radiation-induced lung toxicity (RILT). In a clinical situation, RILT manifests as respiratory distress and changes on thorax radiograph and computed tomography (1).

Several treatment-related factors such as the radiation dose and amount of irradiated lung tissue correlate with the risk of developing RILT (1). In addition to lung tissue, part of the heart is often also irradiated (2). Although the heart is generally considered not to be functionally affected early after irradiation, early radiation-induced effects have been reported in animal (3) and clinical (4) studies. Coirradiation of the heart was also shown to enhance the risk of RILT both in animal studies (5, 6) and in patients with non-small cell lung cancer (NSCLC) (2). Therefore, the contribution of the heart as well as the lung in the development of early RILT should be taken into account for treatment optimization. Until now, however, the mechanism through which this interaction takes place is not known.

Recently, it was shown in rats that lung irradiation induces pulmonary hypertension and right ventricle hypertrophy in an irradiated-volume-dependent manner (7). Pulmonary hypertension can contribute to cardiac dysfunction (8). The possible contribution of radiation-induced pulmonary hypertension in cardiac damage was suggested in the early 1990s in a canine model (9); however, the underlying physiological changes remain unknown.

Taken together, these observations indicate that lung irradiation can cause changes in the heart and that heart irradiation can cause changes in the lung, leading collectively to physiological changes in the cardiopulmonary system. Therefore, in this study we investigated whether physiological changes caused by irradiation of the lung, heart, or both can explain their interaction in the development of radiation-induced cardiopulmonary dysfunction.

Methods and Materials

Animals

Adult male Wistar rats were used. The experiments were performed in agreement with the Netherlands Experiments on Animals Act (1977) and the European Convention for the Protection of Vertebrate Animals Used for Experimental Purposes (Strasbourg, 18.III.1986).

Irradiation technique

Rat hearts, lungs, or both were irradiated (single fraction) using a high-precision proton beam (150 MeV) as described previously (6). Briefly, high-energy protons were used, leading to uniform dose distributions in the longitudinal direction (1%) with sharp lateral field edges (20%-80% isodose distance: 1 mm). This steep penumbra (0.9-1.1 mm) facilitates the separate irradiation of lung and heart required for dissecting the individual contributions of each on tissue damage and dysfunction. The rats were irradiated under anesthesia (isoflurane) and suspended from their incisors. The isodose curves of the irradiation portals (Supplementary Table S1) are shown in Fig. 1.

Breathing rate assay

In preclinical studies, breathing rate (BR) is considered a surrogate measure for pulmonary function (7). The increase of the postirradiation BR relative to the mean BR in weeks 0-2 after irradiation was used as an indicator of early pulmonary dysfunction (7). Current data ($n=5$/group) were combined with historical data (5, 6).

Radiology

Electrocardiogram (ECG)-gated cardiac ^{18}F-fluoridedeoxyglucose positron emission tomography (^{18}F-FDG-PET) scans were used to investigate whether heart irradiation induces cardiac changes. Reduction in ^{18}F-FDG uptake of the left ventricle (LV) was scored (Supplementary Table S2; $n=6$/group) and reported as LV ^{18}F-FDG uptake defect.

Hemodynamic measurements

LV or right ventricle (RV) hemodynamic measurements were carried out to investigate cardiac physiological changes 8 weeks after irradiation. For LV hemodynamic measurement ($n=5$/group), a pressure catheter was introduced via the carotid artery and guided through the aorta into the LV to obtain LV end-diastolic pressure (LVEDP) and Tau (LV relaxation constant). RV pressure and pulmonary artery pressure ($n=4$/group) were recorded from RV hemodynamic measurement (7). Wet lungs were weighed to check if they were edematous. The heart was divided into atria, ventricles, and septum and weighed separately to assess RV hypertrophy (7).

Morphological changes

Pulmonary edema, inflammation and fibrosis, as well as cardiac perivascular fibrosis, were assessed in samples from the irradiated and the shielded lung and heart ($n\geq4$/group). Pulmonary edema was assessed using hematoxylin and eosin staining and semi-quantitative scoring of interstitial and perivascular edema. For interstitial edema, scores from 0-3 were given reflecting the severity of the damage to the interstitial tissue and the amount of affected tissue with or without interstitial infiltrate. For perivascular edema, scores from 0-2 were given to show the severity of the edema around vessels. At least 5 large vessels (>100 μm) and 20 small vessels (<100 μm) with or without perivascular infiltrate were scored. Using hematoxylin and eosin staining, pulmonary

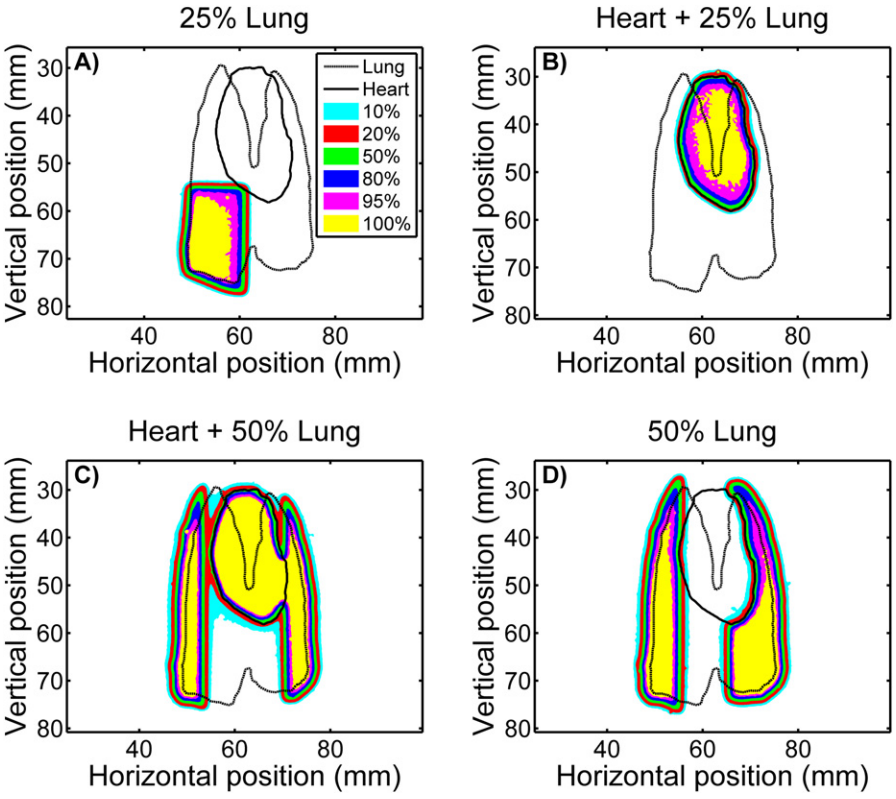

Fig. 1. Isodose contours and anatomy. Colored areas indicate dose, and the solid and dashed contour indicate the outlines of the heart and lung, respectively.

parenchymal inflammation was scored from 0-3 on the basis of the number of inflammatory cells in the lung parenchyma. For fibrosis, Masson trichrome staining was used. Pulmonary parenchymal fibrosis was scored 0-3 based on the amount of deposited collagen. Cardiac perivascular fibrosis was quantified by calculating the ratio of the fibrosis area surrounding the vessel to the total vessel area using an image analysis system (CZ KS400; Imaging Associates, Bicester, United Kingdom). For this, at least 20 vessels were examined, and, depending on the amount of vessels, the average results per group were obtained from LVs of at least 4 rats.

Quantitative polymerase chain reaction

Total RNA was extracted from the phosphate buffered saline-perfused rat LVs (n = 4/group), and cDNA was generated subsequently according to the manufacturers' protocols. Bio-Rad IQTM SYBR Veenendaal, The Netherlands Green Supermix was used to perform amplifications in a Bio-Rad IQ iCycler machine as described by the manufacturer. The following primers were used to amplify fibronectin: 5′-agaccatacctgccgaatgtag and gagagcttcttgtcctgtagag. The mRNA levels were normalized using 36B4 (ribosomal) primers with the sequences 5′-gttgcctcagtgcctcactc and 5′-gcagccgcaaatgcagatgg.

Statistical analysis

Differences between groups were tested by comparing the functional and physiological parameters of the groups using 1-way analysis of variance with Bonferroni post hoc analysis to correct for multiple comparisons. For morphologic assessments, nonparametric Kruskal-Wallis test was performed. P values $< .05$ were considered statistically significant. To determine to what extent the physiological changes could be explained by changes in the morphology, Pearson's product-moment correlation coefficient was used. A correlation was considered significant if the hypothesis of no correlation was rejected at $P<.05$.

More details can be found in the Supplementary Material.

Results

Radiation induces early cardiac damage

To confirm the interaction between lungs and heart on radiation-induced pulmonary dysfunction (5), we investigated the BR after partial irradiation of the rat lung, with or without irradiation of the heart. Coirradiation of the heart induced a pronounced BR increase (Supplementary Fig. S1). This suggests that heart irradiation may induce early subclinical heart damage that manifests only in combination with lung irradiation resulting in an aggravated reduction in lung function (5). To determine whether heart irradiation induces early cardiac damage, cardiac metabolism was assessed by ^{18}F-FDG-PET scans. Scans were taken biweekly for 12 weeks after irradiation of the heart and the adjacent lung tissue (25% of the lung) with a dose below and above 18 Gy, the threshold for lung-heart interaction (6). Indeed, a significant defect in ^{18}F-FDG uptake was observed in the LVs at both dose levels (Fig. 2, $P<.01$ H + 25% L, 16 Gy vs control and $P<.001$ H + 25% L, 25 Gy vs control).

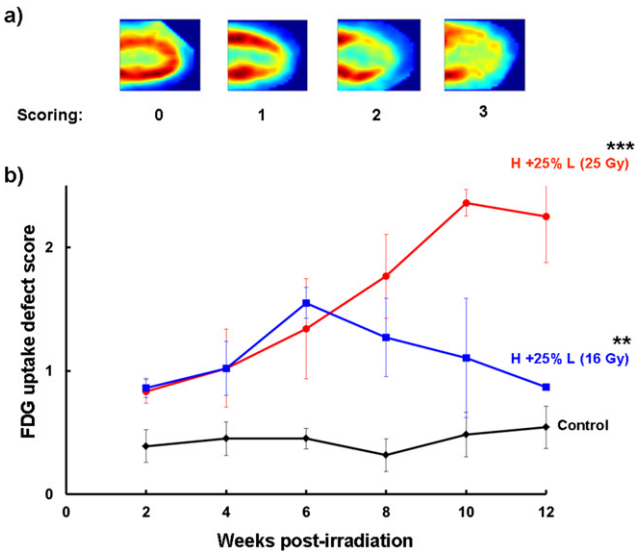

Fig. 2. Cardiac metabolic changes after heart irradiation. Scoring of reduced ^{18}F-fluorodeoxyglucose positron emission tomography (^{18}F-FDG) uptake in irradiated hearts at diastolic phase (week 2-12 postirradiation) (a) shows ^{18}F-FDG uptake defect in irradiated left ventricles to 16 and 25 Gy with more pronounced effect in 25 Gy (b). The areas under the curves (week 2-12) were compared. ***P<.001, **P<.01, *P<.05 compared with control. Data are presented as mean ± SEM.

Heart irradiation induces cardiac fibrosis and myocardial damage

To investigate the origin of these metabolic changes, we investigated the morphology of the LVs. Immunohistochemical staining (Fig. 3a) and morphologic quantification (Fig. 3b, P<.01) showed pronounced perivascular fibrosis in the irradiated LVs (20 Gy). Moreover, in irradiated LVs, a relative increase in fibronectin mRNA expression, a well-established profibrotic gene (10), was observed (Fig. 3c, P<.05).

Aside from perivascular fibrosis, contraction bands (Fig. 3d, yellow arrows) were observed in the myocardium of the irradiated LVs located predominately in endocardium and epicardium.

Heart irradiation induces left ventricle diastolic dysfunction

Myocardial damage and perivascular fibrosis are known to be an important pathophysiological processes contributing to diastolic dysfunction by impairing cardiac relaxation (11, 12). Therefore, we next investigated whether the observed histopathology and metabolic changes translate into changes in cardiac function. To this end, LV hemodynamics were assessed. Heart irradiation (20 Gy) induced a pronounced elevation of the LVEDP (Fig. 4a, P<.05). Moreover, pericardial effusion was observed in 2 of 9 irradiated hearts. Next we determined to what extent radiation-induced physiological changes can be explained by LV morphologic changes, by correlating LV perivascular fibrosis with LVEDP. The perfect correlation (Supplementary Fig. S2a) indicated that LV diastolic dysfunction can be fully explained by changes in cardiac vasculature.

Heart irradiation enhances lung tissue damage

Because diastolic dysfunction is known to promote pulmonary edema (13), it may be the mechanism through which heart irradiation induces pulmonary dysfunction. If so, this would lead to pulmonary edema in shielded lung tissue. Morphologic analysis showed significant pulmonary interstitial edema after heart irradiation (Fig. 5a, P<.001). Moreover, the wet weight of the lungs was higher when the hearts were irradiated (Supplementary Fig. S3). Also in 3 of 9 rats with irradiated hearts (20 Gy), pleural effusion was observed. A strong correlation between LVEDP and pulmonary interstitial edema (Supplementary Fig. S2a) suggests that LV diastolic dysfunction induces secondary lung damage. In addition to pulmonary edema, morphological evaluation revealed more pulmonary parenchymal inflammation and fibrosis (Fig 5b, P<.001 and P<.01 respectively) when the heart was coirradiated.

Combined lung and heart irradiation: double trouble

If irradiation of heart and lung both have a common consequence, this would explain the observed interaction between them. Importantly, irradiation of 50% of lung (20 Gy) has also been shown to induce not only pulmonary edema (Fig. 5a, Supplementary Fig. S3, P<.05) and inflammation (Fig. 5b, P<.05) but also affect the heart due to increased pulmonary tension, leading to RV systolic pressure overload and RV hypertrophy (7) (Supplementary Fig. S4). Because all of these factors are known to cause LV dysfunction (8), we investigated LV function after lung irradiation. Indeed, significant elevation of tau (Fig. 4b, P<.05) was observed. A strong correlation among pulmonary hypertension, perivascular edema, and tau (Supplementary Fig. S2b) indicates that secondary cardiac damage can be explained by radiation-induced lung damage.

We next investigated whether combining these effects by simultaneous irradiation of both organs results in enhanced response. To this end, cardiac performance was assessed after heart + 50% lung irradiation (20 Gy). Significant elevation of both LVEDP (Fig. 4a, P<.01) and tau (Fig. 4b, P<.05), in addition to perivascular fibrosis (Fig. 3b, P<.001) were observed in this setting. Furthermore, enhanced wet lung weight increase (Supplementary Fig. S2, P<.001), pulmonary interstitial edema (Fig. 5a, P<.001), perivascular edema (Fig. 5a, P<.05), parenchymal inflammation (Fig. 5b, P<.001), fibrosis (Fig. 5b, P<.001), and pleural effusion (5 of 9 rats) were observed in the group that received combined lung and heart irradiation. In addition to LV diastolic dysfunction, pulmonary edema may also develop from RV diastolic dysfunction, because it may be induced by pulmonary hypertension (Supplementary Fig. S4a and S4b). Consistent with this, we also observed a pronounced increase in RV diastolic pressure (Fig. 6, P<.001).

Discussion

Our results document the physiology of how cardiac and pulmonary damage can mutually influence cardiopulmonary function. We observed that heart irradiation directly affects cardiac vasculature and myocardium and therefore increases end-diastolic pressure, leading to LV diastolic dysfunction, which promotes

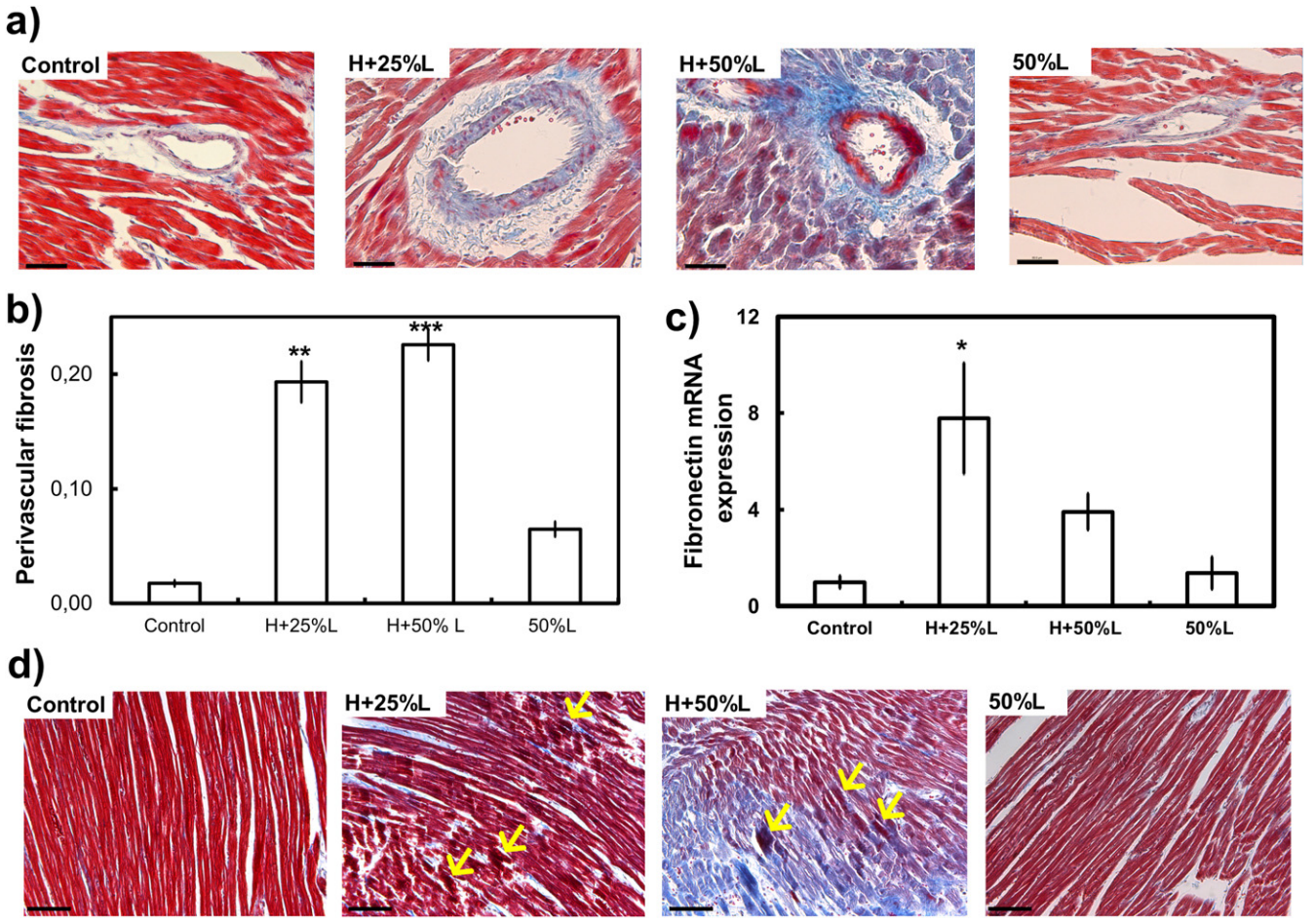

Fig. 3. Left ventricular perivascular fibrosis and myocardial damage in irradiated hearts, observed by immunohistochemical staining (a, d), morphologic quantification of perivascular fibrosis (b), and relative fibronectin mRNA expression (c). Contraction bands (d, shown by yellow arrows) were observed in the epicardium and endocardium of the irradiated hearts. Scale bars on panel a, d, and e represent 50 μm, 1 mm, and 100 μm, respectively. Masson trichrome staining was performed: red stain = muscle fiber, blue stain = collagen. ***$P<.001$, **$P<.01$, *$P<.05$ compared with control. Data are presented as mean ± SEM.

pulmonary interstitial edema. Lung irradiation indirectly impairs LV diastolic function through radiation-induced pulmonary hypertension, pulmonary perivascular edema, and the resultant effect on LV relaxation time. Combined lung and heart irradiation enhances cardiac diastolic dysfunction via both mechanisms, which may result in biventricle dysfunction, explaining the observed aggravated cardiopulmonary dysfunction. We propose that cardiac dysfunction, either originating directly from heart irradiation or indirectly caused by lung irradiation, may be an important factor causing or enhancing cardiopulmonary toxicity after thoracic radiation therapy.

Consistent with our observations, changes in cardiac ^{18}F-FDG uptake were observed in patients with esophageal cancer 3-9 months postradiation therapy. Moreover, these changes correlated

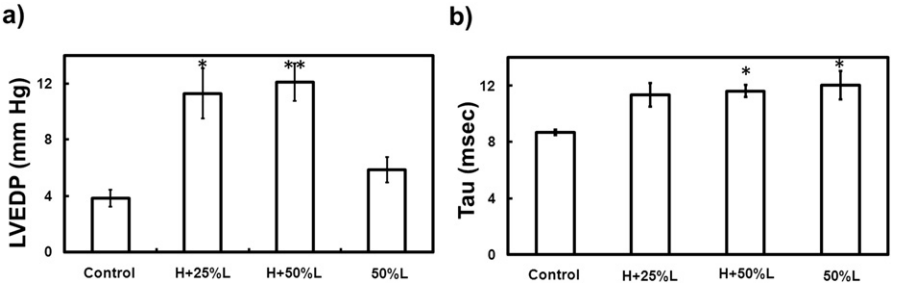

Fig. 4. Left ventricular hemodynamics after heart or lung irradiation, or both. Significant increases in LV end-diastolic pressure (LVEDP) were observed in H + 25% L and H + 50% L groups (a), whereas elevation of tau was observed in 50% L and H + 50% L groups (b). ***$P<.001$, **$P<.01$, *$P<.05$ compared with control. Data are presented as mean ± SEM.

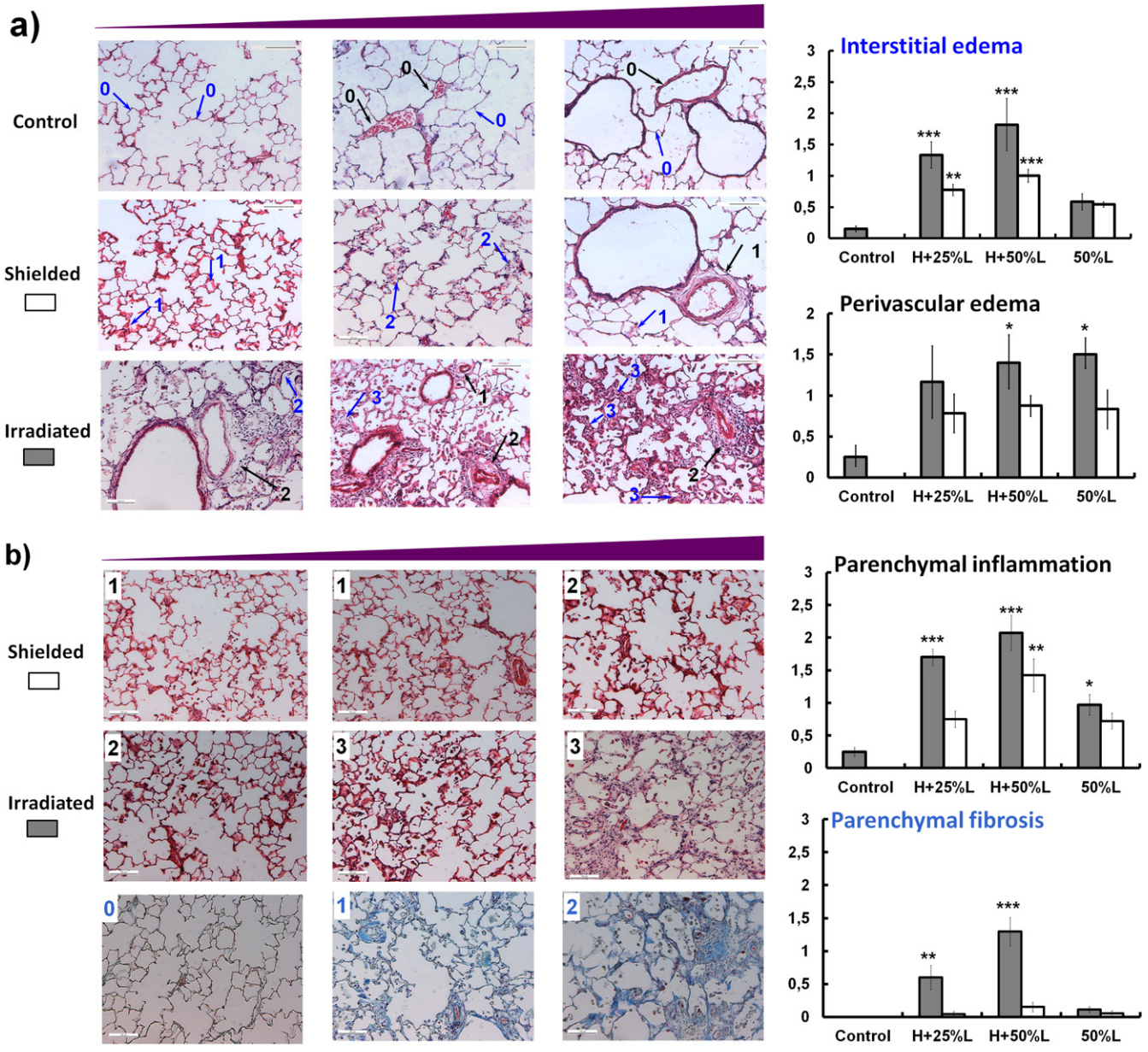

Fig. 5. The morphology of the lung after heart or lung irradiation, or both. (a) Semiquantitative scoring of pulmonary interstitial (blue arrows) and perivascular edema (black arrows). The numbers in the pictures show the given scores (interstitial edema: blue, perivascular edema: black). The first, second, and third rows show representative examples of the lung tissue taken from nonirradiated controls, shielded and irradiated parts, respectively. From left to right, columns show increasing levels of the tissue damage. Significant increase of global pulmonary interstitial edema was observed when the heart was coirradiated with the lungs. Fifty percent lung irradiation with or without coirradiation of the heart significantly increased pulmonary perivascular edema. (b) The first and second rows show semiquantitative scoring of parenchymal inflammation in representative examples of the lung tissue taken from shielded and irradiated parts respectively (hematoxylin and eosin staining). The third row shows semiquantitative scoring of parenchymal fibrosis in the lung tissue. The numbers on the left upper corner of the pictures show the given scores (inflammation: black; fibrosis: blue). Coirradiation of the heart significantly increased the number of inflammatory cells and the amount of deposited collagen in the lung tissue. Lung irradiation alone significantly increases the number of inflammatory cells. Scale bar shows 100 μm. The purple bar shows increasing the level of tissue damage. ***$P<.001$, **$P<.01$, *$P<.05$ when compared with control. Data are presented as mean ± SEM.

with elevated plasma levels of brain natriuretic peptide, a known marker of cardiac diastolic dysfunction in patients with acute dyspnea (14).

In preclinical studies on RILT, BR increase is often considered a surrogate measurement of radiation pneumonitis (1). Indeed, these BR changes may reflect a reduced diffusion capacity due to parenchymal damage such as alveolitis. In addition, it may reflect decreased ventilation efficiency as a consequence of reduced perfusion, a symptom frequently observed in patients with pulmonary hypertension and edema (7). Radiation-induced pulmonary hypertension was shown to contribute to BR changes not only in single irradiation dose preclinical studies (7, 9) but also

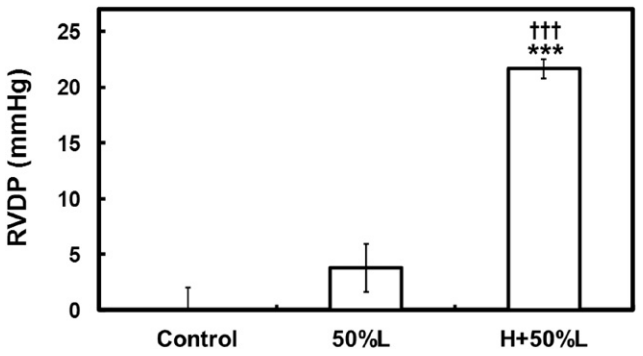

Fig. 6. Right ventricular (RV) hemodynamics after irradiation of the heart and 50% of the lung. A dramatic elevation of RV diastolic pressure (RVDP) was observed. ***$P<.001$ (H + 50% L vs Control), $^{\dagger\dagger\dagger}P<.001$ (H + 50% L vs 50%). Data are presented as mean ± SEM.

in fractionation study in a canine model (15). Clinical symptoms of cardiac diastolic dysfunction are also predominantly respiratory in nature due to backward failure of the LV causing congestion of the pulmonary vasculature and pulmonary edema (13). Consistent with this, cardiac dysfunction was shown to play key role in the development of BR increase in our study. Taken together, this suggests that dyspnea may originate from physiological cardiopulmonary changes such as cardiac diastolic dysfunction and pulmonary hypertension rather than parenchymal damage alone. However, to substantiate our findings, studies with fractionated dose in larger animal models or in patients should be performed.

Current practice in the optimization of the treatment of NSCLC is mainly based on the dose distribution in the lungs and the dose to spinal cord. The local control of the lung tumors could be improved to ~80%-90% by increasing the tumor dose by ~20% (16). At present, however, this dose escalation is not possible in the majority of patients because of the associated risk of RILT. Importantly, in our preclinical studies, differences in tolerance dose between coirradiating and sparing of the heart were typically in the same range (5, 6). Currently, conforming to the dose constraints of the lung often results in an increase of dose to the heart. Our present work shows that for a given lung dose, increasing dose to the heart may in fact increase the risk of RILT, thus hampering efforts for dose escalation. Therefore, adding dose constraints for the heart in the treatment optimization for NSCLC may allow dose escalation and consequently increase the local control. Recently, preclinical and clinical studies have suggested that models of RILT can be improved by accounting for the impact of dose to the heart on the risk of complications (2, 6). However, the approach to optimally distribute dose over the lung and heart is still unclear. Because we now show that symptomatic RILT results from physiological cardiopulmonary changes, dose-response relationships of these changes such as LVEDP and pulmonary artery pressure in patients incorporating both lung and heart dose-volume variables are needed to build more accurate predictive models.

In addition to dosimetric factors, pretreatment clinical factors could be incorporated into the predictive models. Preexisting lung diseases (17) and cardiac and pulmonary comorbidity (18) are known to predict adverse effects of a treatment. More accurate models will help to identify patients with a higher risk of RILT. Notably, dose limits for the entire population is currently based on these patients, accurately identifying them increases the tolerance of the residual population, thereby allowing tumor dose escalation. The patients for whom tumor location and size prevents radiation therapy with conventional modalities are suitable candidates for dose escalation by more focalized radiation treatment modalities such as particle radiation therapy (19). Here, the dose is more confined to the target, and coirradiation of the heart and large volumes of healthy lung tissue can be more effectively spared (19).

Symptoms of RILT were shown not to be limited to patients with radiologic changes, nor were these changes exclusively associated with symptomatic patients (20). Radiographically occult factors such as vascular damage (7) and cardiac damage (present results) may contribute to the development of RILT and the associated symptoms. Therefore, in addition to diagnostic tools of lung damage, (subclinical) cardiac damage should be assessed for a better assessment of RILT.

Taken together, our findings show for the first time that reducing the risk of the multiorgan complication RILT, requires specific optimization of the treatment with respect to cardiac and pulmonary dose. This may lead to the development of more accurate prediction and more effective treatment of thoracic cancers, thereby facilitating individualized dose escalation, increased local control, and improved quality of life for patients undergoing thoracic radiation therapy.

References

1. Marks LB, Yu X, Vujaskovic Z, et al. Radiation-induced lung injury. *Semin Radiat Oncol* 2003;13:333-345.
2. Huang EX, Hope AJ, Lindsay PE, et al. Heart irradiation as a risk factor for radiation pneumonitis. *Acta Oncol* 2011;50:51-60.
3. Lauk S. Endothelial alkaline phosphatase activity loss as an early stage in the development of radiation-induced heart disease in rats. *Radiat Res* 1987;110:118-128.
4. Marks LB, Yu X, Prosnitz RG, et al. The incidence and functional consequences of RT-associated cardiac perfusion defects. *Int J Radiat Oncol Biol Phys* 2005;63:214-223.
5. van Luijk P, Novakova-Jiresova A, Faber H, et al. Radiation damage to the heart enhances early radiation-induced lung function loss. *Cancer Res* 2005;65:6509-6511.
6. van Luijk P, Faber H, Meertens H, et al. The impact of heart irradiation on dose-volume effects in the rat lung. *Int J Radiat Oncol Biol Phys* 2007;69:552-559.
7. Ghobadi G, Bartelds B, van der Veen SJ, et al. Lung irradiation induces pulmonary vascular remodeling resembling pulmonary arterial hypertension. *Thorax* 2012;67:334-341.
8. Marcus JT, Gan CT, Zwanenburg JJ, et al. Interventricular mechanical asynchrony in pulmonary arterial hypertension: Left-to-right delay in peak shortening is related to right ventricular overload and left ventricular underfilling. *J Am Coll Cardiol* 2008;51:750-757.
9. Gillette SM, Powers BE, Orton EC, et al. Early radiation response of the canine heart and lung. *Radiat Res* 1991;125:34-40.
10. Crawford DC, Chobanian AV, Brecher P. Angiotensin II induces fibronectin expression associated with cardiac fibrosis in the rat. *Circ Res* 1994;74:727-739.
11. Mann DL. Mechanisms and models in heart failure: A combinatorial approach. *Circulation* 1999;100:999-1008.
12. Miyazaki S, Fujiwara H, Onodera T, et al. Quantitative analysis of contraction band and coagulation necrosis after ischemia and reperfusion in the porcine heart. *Circulation* 1987;75:1074-1082.
13. Grossman W. Diastolic dysfunction in congestive heart failure. *N Engl J Med* 1991;325:1557-1564.
14. Ritchie RH, Rosenkranz AC, Kaye DM. B-type natriuretic peptide: Endogenous regulator of myocardial structure, biomarker and therapeutic target. *Curr Mol Med* 2009;9:814-825.

15. Poulson JM, Vujaskovic Z, Gillette SM, et al. Volume and dose-response effects for severe symptomatic pneumonitis after fractionated irradiation of canine lung. *Int J Radiat Biol* 2000;76: 463-468.
16. Bradley J, Graham MV, Winter K, et al. Toxicity and outcome results of RTOG 9311: A phase I-II dose-escalation study using three-dimensional conformal radiotherapy in patients with inoperable non-small-cell lung carcinoma. *Int J Radiat Oncol Biol Phys* 2005;61: 318-328.
17. Marks LB, Munley MT, Bentel GC, et al. Physical and biological predictors of changes in whole-lung function following thoracic irradiation. *Int J Radiat Oncol Biol Phys* 1997;39:563-570.
18. Charlson ME, Pompei P, Ales KL, et al. A new method of classifying prognostic comorbidity in longitudinal studies: Development and validation. *J Chronic Dis* 1987;40:373-383.
19. Zhang X, Li Y, Pan X, et al. Intensity-modulated proton therapy reduces the dose to normal tissue compared with intensity-modulated radiation therapy or passive scattering proton therapy and enables individualized radical radiotherapy for extensive stage IIIB non-small-cell lung cancer: A virtual clinical study. *Int J Radiat Oncol Biol Phys* 2010;77:357-366.
20. Jenkins P, Welsh A. Computed tomography appearance of early radiation injury to the lung: Correlation with clinical and dosimetric factors. *Int J Radiat Oncol Biol Phys* 2011.